

Photocatalytic TiO₂ Embedded on PET-g-PAAC Fabric by Sono-gamma Irradiation Technique

SHEIKHA A. ALKHURSANI^{1,*}, MOHAMED MADANI¹ and MOHAMED MOHAMADY GHOBASHY^{2,*}

¹Faculty of Science and Humanities-Jubail, Imama Abdulrahman Bin Faisal University, Jubail, Saudi Arabia

²Radiation Research of Polymer Department, National Center for Radiation Research and Technology (NCRRT), Atomic Energy Authority, P.O. 29, Nasr City, Cairo, Egypt

*Corresponding authors: E-mail: salkhursani@iau.edu.sa; mohamed.ghobashy@eaea.org.eg

Received: 8 August 2019;

Accepted: 30 September 2019;

Published online: 30 December 2019;

AJC-19725

Fabrication of photocatalytic TiO₂ particles onto PET-g-PAAC fabric has been succeeded by ultrasonic-gamma irradiation methods. Ultrasonic irradiation assisted for good distribution of TiO₂ particles onto the surface of PET fabric in a uniform manner at ambient conditions. The product modify PET fabric was characterized by attenuated total reflection-Fourier transform infrared (ATR-FTIR) confirmed the grafting of COOH groups onto PET fabric. SEM images revealed a good dispersed and adherent obtained TiO₂ particle onto PET fabric. Results obtained from X-ray diffraction indicating TiO₂ (Degussa P25) in the anatase and rutile phases. The degradation process of three different dyes remazol red, amido black and toluidine blue from aqueous solutions by TiO₂@PET-g-PAAC was investigated using modified photo reactor. It was found that decolorization of toluidine blue was 99 % after 60 min. The reused of TiO₂@PET-g-PAAC showed that the activity of TiO₂@PET-g-PAAC for degradation still remained good which conclude that PET fabric makes TiO₂ easily recovered, which overcomes the disadvantage of separation difficulty of common catalyst after or through degradation processing.

Keywords: Polymer formation, Surface modification, Fabrication composites, PET fabric, Grafting, Gamma-Radiation.

INTRODUCTION

Removal of organic pollutants from water has been considered as one of the serious challenges facing the worldwide. Recently, metal oxide semiconductors nanoparticles can be used to remove the organic pollutants by decomposing dye when exposure to light with a certain wavelength resulting in CO₂ and H₂O. Photocatalytic degradation using TiO₂ is a well known method for removing organic pollutants [1], it is non-toxic, chemically stable, cheap and efficient. Titanium dioxide (TiO₂) is very interesting for a wide range of applications such as photovoltaic cells, gas sensors, heterogeneous photocatalysis and photoelectrochromic devices [2]. Its high photoefficiency and stability under UV illumination enable as one of the most active and promising heterogeneous photocatalysts for the removal of undesirable organic contaminants in wastewater. The photoactivity of TiO₂ is strongly dependent on its crystalline structure, crystallite size and the surface area [3]. TiO₂ in the anatase crystalline form appears to be the most photoactive [4].

However, high dispersion of TiO₂ in water restricts its re-usability. The embedded of TiO₂ onto PET fabric becomes necessary [5]. Combination of TiO₂ with magnetic oxide results in more efficient photocatalytic degradation reaction [6]. Fenton reactions [7] or photo-Fenton reactions [8] using ferric oxide are new methods for dye removal. Coating grafting fabric by polymer is useful and able to withstand highly oxidative radicals produced by embedded TiO₂, which exhibit stable performance during long-term operation. This process avoid TiO₂ leaching from the polymer surface within the reaction and also provide acceptable kinetics during the photocatalytic process [9]. In this connection, TiO₂@PET-g-PAAC fabric as photocatalysts successfully synthesized using sono-gamma irradiations techniques. The fabrication of TiO₂ photocatalyst includes thermal hydrolysis, sol-gel, template process, thermal oxidation, chemical-precipitation, microemulsion process and hydrothermal processing [10,11] is often complex and performs at high temperatures lead to decrease the efficiency of catalyst. In order to eliminate these limitations, ultrasound can be used as an energy source.

Sonochemistry has been successfully used for the fabrication and modification of nanosized functional inorganic materials [12-15]. The chemical effects of ultrasound arise from acoustic cavitations that are the formation, growth and collapse of bubbles in liquid [16]. The generated hot spots can cleave water molecules to produce hydroxyl radical ($\cdot\text{OH}$) which is a powerful oxidant [17].

Fibers have been produced from a wide range of polymers for clothing and household items [18]. PET fabrics are produced by a melt or solution spinning process, which results in oriented materials [19,20]. PET fabrics are used in many applications including packaging [21] and electronic recording [22], chemical sensors [23] and in membranes for many separations applications [24] and water purification [25]. In this work, ultrasound and gamma-irradiation have been applied in the fabrication of TiO_2 @PET-g-PAAc for the photocatalytic applications. The radiation grafting of acrylic acid monomer [26] onto PET fabric was carried out in an ambient conditions to enhance of day absorbance on PET surface. In addition, ultrasonic irradiation could help in grafting process and distribution of TiO_2 onto the surface of PET fabric as performed by SEM and XRD. The efficiency of photocatalyst was examined for three dyes (amido black, remazol red and toluidine blue), the result confirmed the high catalytic activity expected of TiO_2 @PET-g-PAAc.

EXPERIMENTAL

Acrylic acid monomer (AAc) was obtained from Merck Chemical Co. Darmstadt, Germany. Titanium dioxide (TiO_2) (Degussa p25) and PET fabric are the gifted samples. Remazol red an azo-reactive dye was obtained from DyStar, Germany. Toluidine Blue, a basic thiazine metachromatic dye and amido black, amino acid diazo dye were procured from Sigma-Aldrich (U.S.A.).

Gamma irradiation cell: Irradiation to the required doses was carried out in the cobalt-60 gamma cell facility of National Center for Radiation Research and Technology (NCRRT), Atomic Energy Authority of Egypt, Cairo, Egypt. The cobalt-60 gamma cell was made in India and the irradiation was carried out at a dose rate of 2.02 kGy/h.

Modification of polyethylene terephthalate (PET) fabric surface belong with *in situ* deposition and grafting of TiO_2 and PAAc under ultrasonic and gamma-irradiation.

As mention earlier [27], the surface modification of PET was carried out in two steps. Firstly, 2 mL of AAc monomers and 0.01 g of TiO_2 (Degussa P25) were added to 50 mL distilled water and sonicated for 10 min at ambient temperature. Followed that a piece of PET fabric (2 cm \times 2 cm) was immersed to a mixture solution. The reaction mixture was continued sonication for 10 min. Secondly, modified PET fabric was removed from mixture and exposed to gamma-radiation for dose of 5 kGy at ambient condition to complete the grafting of PAAc on PET fabric. Finally, TiO_2 @PET-g-PAAc was sonicated for 20 min followed by drying at room temperature. The grafting of AAc might by sonication and gamma irradiation both of them leads to water sonolysis and waterradiolysis for given hydroxyl and per hydroxyl radical.

Catalytic activity of TiO_2 @PET-g-PAAc: Decolourization of three dyes (amido black, remazol red and toluidine blue)

in aqueous solution were performed at the ambient temperatures. Obtained TiO_2 @PET-g-PAAc (0.90 g) was placed and mixed with 2×10^{-5} M of dyes in a 20 mL deionized water for 30 min in a dark and allowed to reach adsorption equilibrium before the irradiation. A photocatalytic degradation of three dyes by TiO_2 @PET-g-PAAc was carried out under irradiation of a light source UV lamp irradiation range of 28 W at $\lambda = 362$ nm and fluorescent lamp 8 W at range of $\lambda = 375$ -750 nm, the mixture of dye and catalyst was sampled at different interval of times.

Again, an aliquot of 3 mL of dye solution was taken from the reactor at regular interval of time (10 min). The sample was analyzed by UV-Vis spectrophotometer to determine the of concentration of three dyes at λ_{max} of 530 (for remazol red), 620 (for amido black) and 585 nm (for toluidine blue). Then, absorption spectrum (eqn. 1) obtained through absorption peak decay at UV-Vis spectrophotometer for the decolourization of three dyes.

$$\text{Decolourization (\%)} = \frac{C_0 - C}{C_0} \times 100 \quad (1)$$

where C_0 is the initial concentration of dye and C is the concentration of dye at specified time.

Photodegradation: The samples were exposed to UV irradiation of 28 W at 362 nm and fluorescent lamp 8 W at range of 375-750 nm. Eliminated the heat effect of the lamps by cooling fan, thus the temperature of the reaction medium was maintained constant at 20 ± 0.1 °C. The intensity of irradiation entering the beaker is homogeny by positing up of UV lamp and mirror downs the beakers.

Characterization: Attenuated total reflectance-Fourier transform infrared (ATR-FTIR) Vertex 70 FTIR spectrometer equipped with HYPERION™ series microscope (Bruker Optik GmbH, Ettlingen, Germany) over the 4000-500 cm^{-1} range was used. Software OPUS 6.0 (Bruker) was used for data processing, which was baseline-corrected by the rubber band method with exclusion of CO_2 bands. The dried samples of PET were examined with JEOL JSM-5400 scanning electron microscopy (SEM). The surface of PET fabric was sputter-coated with gold for 4 min. The X-ray diffraction (XRD) patterns of PET and TiO_2 @PET-g-PAAc were recorded on The XRD-6000 series from Shimadzu Scientific Instruments (SSI), Kyoto, Japan. Absorbance values of dyes were measured on UNICAM UV-Vis and 1000 Model spectrophotometers. The various dye samples were kept under normal conditions (ambient temperature in dark).

RESULTS AND DISCUSSION

Chemical composition of TiO_2 @PET-g-PAAc fibers are identified by ATR-FTIR: For identification of PAAc grafted and TiO_2 incorporated onto PET fabric was evaluated by ATR-FTIR spectra are shown in Fig. 1a-b. The ATR-FTIR charts showed that the peaks at 1639 and 1716 cm^{-1} specified for ester and carboxylic groups for PET blank and grafted fibers, respectively. This indication of PAAc was grafted onto PET fiber. In addition many peaks holding to TiO_2 are observed in Fig. 1b. Such as the broad peak in 600 to 450 cm^{-1} region is attributed due to the stretching vibration of Ti-O.

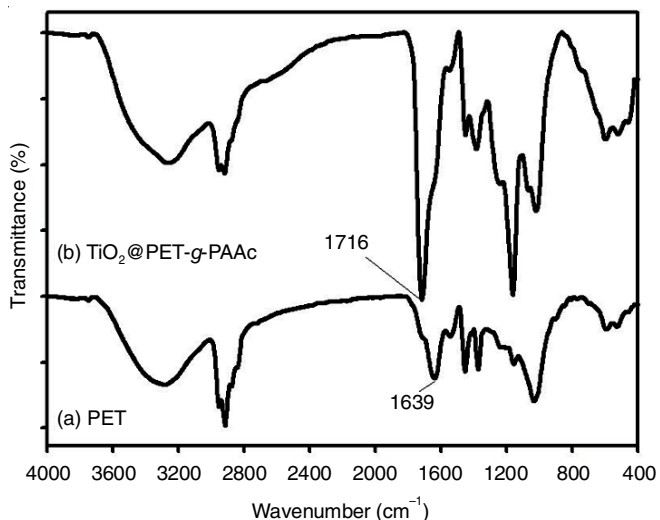


Fig. 1. FTIR spectra for original PET fiber (a) and TiO₂@PET-g-PAAc fabrics (b)

Surface morphology and TiO₂ distribution in PET-g-PAAc fabric: Scanning electron microscopy technique provide more resolvable of a PET fabric surface before and after modification. Fig. 2a shows splits PET fibers with diameter ranged

from 5 to 25 μm . The surface morphology of TiO₂@PET-g-PAAc fabric is shown in Fig. 2b. Dense TiO₂ particles with good distribution can be seen but their size not clear at this magnification.

Fig. 2c shows the cross-sections of loaded PET fabric, which clearly indicated the good adherent of TiO₂ particles onto the PET surface. Also, a dense TiO₂ particles around PET fabrics are observed which resulted from the combined ultrasonic and gamma irradiations. Further, cross section structural study can be conducted by grafted PET fabric (Fig. 2d), where thicker grafted PAAc with TiO₂ are presented significantly (12 μm).

XRD patterns of TiO₂@PET-g-PAAc fabrics: Fig. 3a shows the XRD patterns of PET fabrics, which reveals a semi-crystalline structure with a peak characteristic at $2\theta = 14.32^\circ$, 16.79° , 18.76° , 21.76° and 25.70° , respectively. The PET orientation was changed after PET grafted with PAAc and the peaks were shifted from 14.32° (6.18 \AA) to 14.64° (6.04 \AA), 16.79° (5.21 \AA) to 16.04° (5.52 \AA), 18.76° (4.72 \AA) to 18.81° (4.71 \AA), 21.76° (4.08 \AA) to 21.88° (4.05 \AA) and 25.70° (3.46 \AA) to 25.72° (3.45 \AA). Almost these change for internal planer distance according to graft process. XRD patterns also exhibited strong diffraction peaks at 27° , 36° and 55° indicated that TiO₂ in rutile phase, while the diffraction peaks at 25° and 48°

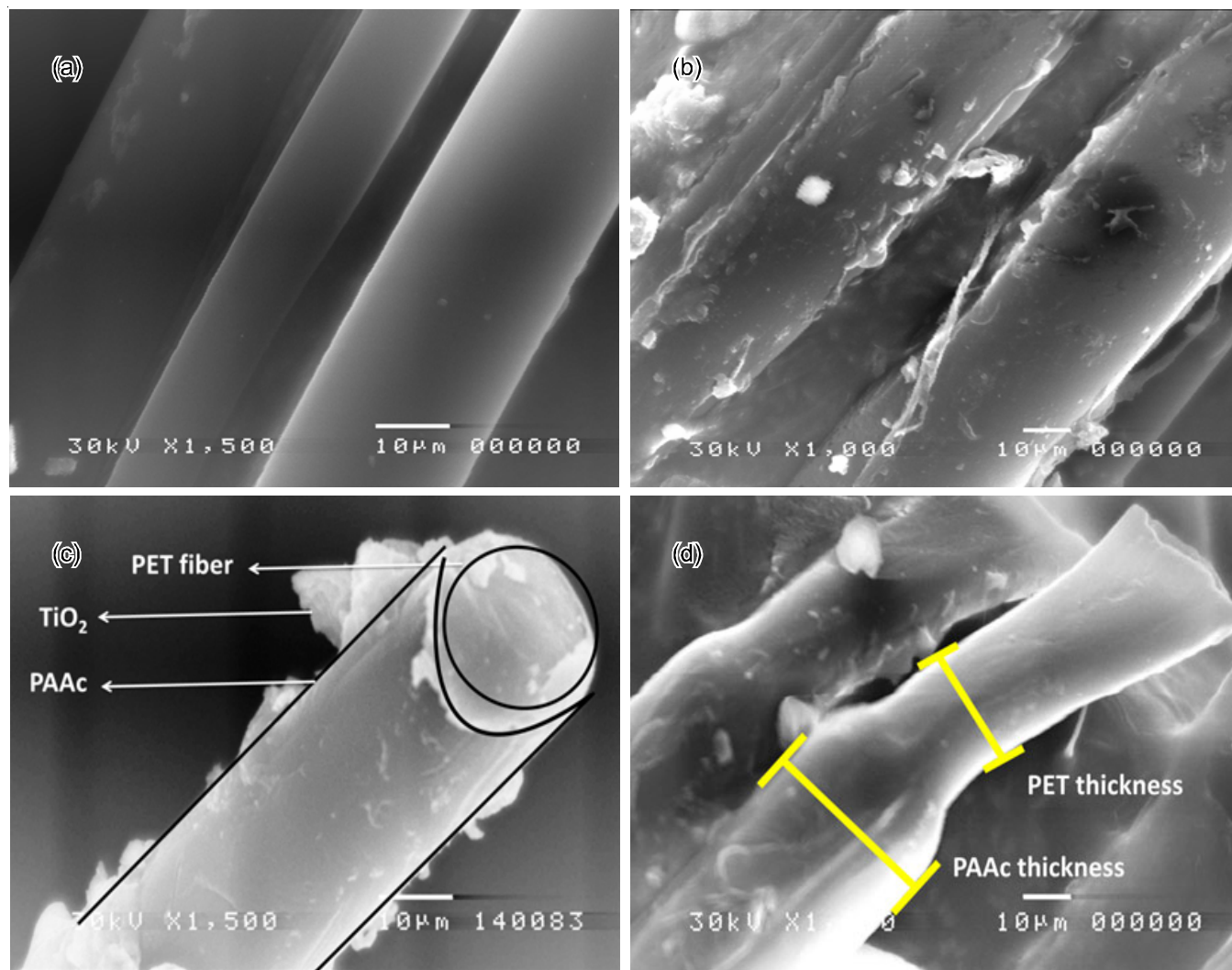


Fig. 2. SEM images of (a) blank PET fabric, (b) TiO₂@PET-g-PAAc, (c) and (d) cross-sections of grafted PET fabric

indicated TiO₂ in anatase phase (Fig. 3b). All the peaks are in good agreement with the standard spectrum (JCPDS no.: 88-1175 and 84-1286) [28]. The peak visible at $2\theta = 42.96^\circ$ represents the presence of iron in PET samples [29], where iron is useful for textile stained process.

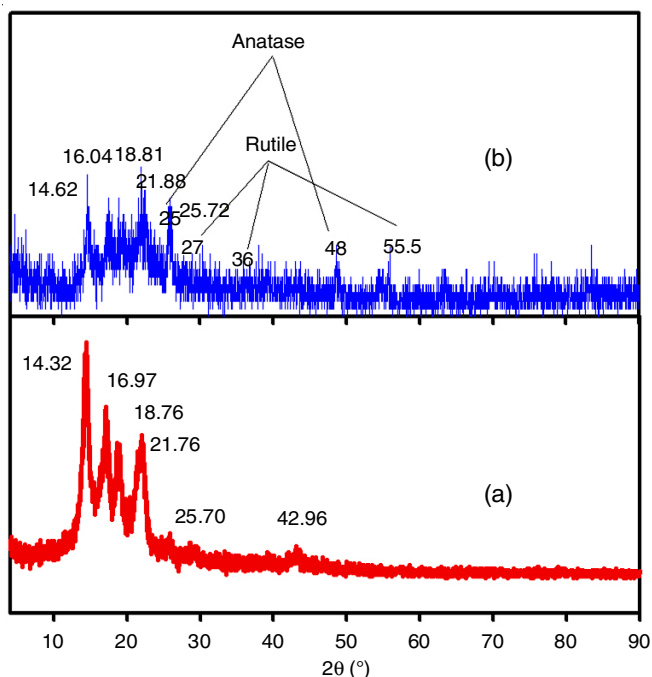


Fig. 3. XRD patterns of (a) PET and (b) TiO₂@PET-g-PAAc

Photocatalytic degradation of dyes by TiO₂ embedded on PET-g-PAAc: Fig. 4 shows the decolourization percentage changes that occurred during the photocatalytic degradation of three dyes *viz.*, amido black, remazol red and toluidine blue at the concentration of 2×10^{-5} M having 0.9 g TiO₂@PET-g-PAAc in 20 mL aqueous solution. As shown in Fig. 4, the decolourization (%) of three dyes with strong absorption band at $\lambda = 530$ nm with different time of intervals. The decolourization (%) is increases as the reaction time increases. After 60 min, the red, deep blue and blue colours were gradually decrease to 17.94, 31.20 and 99.12 % of remazol red, amido black and

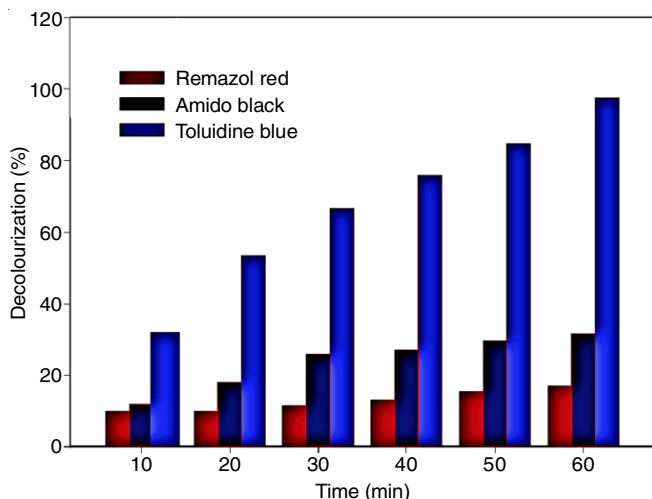


Fig. 4. Rate of decolourization of 2×10^{-5} M remazol red, amido black toluidine blue using and 0.9 g TiO₂@PET-g-PAAc at 30 ± 0.1 °C

toluidine blue, respectively. The decrease of colour intense can be attributed to continuous degradation of dye in the presence of TiO₂ or increased dye absorption due to presence of PAAc. Moreover, reaction time also enhances the diffusion of dyes on the PET chains and accelerates the dye degradation rate onto TiO₂@PET-g-PAAc surface.

Long-term activity of TiO₂ embedded in PET-g-PAAc:

The regeneration of TiO₂ photocatalyst was one of key steps to make heterogeneous photocatalysis technology for practical applications. The separation problem of photocatalyst has been solved without depressing the activity of Degussa P25 by modifying PET with grafted hydrophilic polymer PAAc between the PET and Degussa P25 particles. So, the photocatalyst can be reused easily without any mass loss. The experiments on 0.9 g TiO₂@PET-g-PAAc recycled were carried out under the same reaction conditions. After each reaction cycle, catalyst was separated from the reaction mixture and then reused for the next experiment with fresh adding aqueous solution (20 mL) of toluidine blue. It was observed that even after three cycles, the activity of 0.9 g TiO₂@PET-g-PAAc for degradation still remained good. From first run, it is observed that the decolorization of toluidine blue attained the almost total elimination of toluidine blue (99.9 %) in 60 min. During two cycle, 95 % decolorization of toluidine blue was achieved within 50 min, similarly, during three run, 95 % decolorization of toluidine blue was achieved after 40 min. Thus, it proves the high photocatalytic efficiency of TiO₂@PET-g-PAAc.

Conclusion

Hydrophilic polymer PAAc grafting onto PET fabric believed to increase ability of PET fabric for dyes absorption. As revealed by SEM images, PAAc could responsible for the good adherent of TiO₂ onto the surface of PET fabric. This feature could useful for giving good contact between dyes and TiO₂ catalyst to enhance the degradation process. Among the catalytic degradation of three tested dyes (amido black, remazol red and toluidine blue) showed that the rate of decolourization of toluidine blue is very fast in comparison to others dyes. The durability and longevity of prepared TiO₂@PET-g-PAAc catalyst revealed that the activity of TiO₂@PET-g-PAAc for degradation still remained good even after three runs. Most importantly, this work concluded that PET fabric makes TiO₂ easily recovered which overcomes the disadvantage of separation difficulty of common catalysts after degradation process.

CONFLICT OF INTEREST

The authors declare that there is no conflict of interests regarding the publication of this article.

REFERENCES

1. D. Karamanis, A.N. Ökte, E. Vardoulakis and T. Vaimakis, *Appl. Clay Sci.*, **53**, 181 (2011); <https://doi.org/10.1016/j.clay.2010.12.012>.
2. R. T. Asahi, *Science*, **293**, 269 (2001); <https://doi.org/10.1126/science.1061051>.
3. L. Q. Gao and Q. Zhang, *Scr. Mater.*, **44**, 1195 (2001); [https://doi.org/10.1016/S1359-6462\(01\)00681-9](https://doi.org/10.1016/S1359-6462(01)00681-9).
4. K. M. Schindler and M. Kunst, *J. Phys. Chem.*, **94**, 8222 (1990); <https://doi.org/10.1021/j100384a045>.

5. H. Zhang, H. Zhu and R. Sun, *Text. Res. J.*, **82**, 747 (2012); <https://doi.org/10.1177/0040517511424526>.
6. P. Xu, G.M. Zeng, D.L. Huang, C.L. Feng, S. Hu, M.H. Zhao, C. Lai, Z. Wei, C. Huang, G.X. Xie and Z.F. Liu, *Sci. Total Environ.*, **424**, 1 (2012); <https://doi.org/10.1016/j.scitotenv.2012.02.023>.
7. M.-W. Chang and J.-M. Chern, *J. Taiwan Inst. Chem. Eng.*, **41**, 221 (2010); <https://doi.org/10.1016/j.jtice.2009.08.009>.
8. H. Katsumata, S. Kawabe, S. Kaneco, T. Suzuki and K. Ohta, *J. Photochem. Photobiol. Chem.*, **162**, 297 (2004); [https://doi.org/10.1016/S1010-6030\(03\)00374-5](https://doi.org/10.1016/S1010-6030(03)00374-5).
9. Y. Zhiyong, D. Laub, M. Bensimon and J. Kiwi, *Inorg. Chim. Acta*, **361**, 589 (2008); <https://doi.org/10.1016/j.ica.2007.05.062>.
10. C.J. Ren, B.H. Zhong, D.L. Zhou, H. Liu, D.C. Li and J.H. Gong, *Chinese J. Rare Metals*, **28**, 903 (2004).
11. Y.F. Xiao and S. Liu, *Bull. Chinese Ceramic Soc.*, **26**, 523 (2007).
12. L. W. Zhou, W. Wang, S. Liu, L. Zhang, H. Xu and W. Zhu, *J. Mol. Catal. A*, **252**, 120 (2006); <https://doi.org/10.1016/j.molcata.2006.01.052>.
13. A. Hassani, A. Khataee, S. Karaca, C. Karaca and P. Gholami, *Ultrason. Sonochem.*, **35**, 251 (2017); <https://doi.org/10.1016/j.ultsonch.2016.09.027>.
14. N. Ghows and M.H. Entezari, *Ultrason. Sonochem.*, **18**, 629 (2011); <https://doi.org/10.1016/j.ultsonch.2010.08.003>.
15. L. Mao, J. Liu, S. Zhu, D. Zhang, Z. Chen and C. Chen, *Ultrason. Sonochem.*, **21**, 527 (2014); <https://doi.org/10.1016/j.ultsonch.2013.09.001>.
16. N.A. Dhas and K.S. Suslick, *J. Am. Chem. Soc.*, **127**, 2368 (2005); <https://doi.org/10.1021/ja049494g>.
17. A. M. Khataee, M. Sheydaei, A. Hassani, M. Taseidifar and S. Karaca, *Ultrason. Sonochem.*, **22**, 404 (2015); <https://doi.org/10.1016/j.ultsonch.2014.07.002>.
18. S. Gowri, L. Almeida, T. Amorim, N. Carneiro, A.P. Souto and M.F. Esteves, *Text. Res. J.*, **80**, 1290 (2010); <https://doi.org/10.1177/0040517509357652>.
19. A. Dutta, *Text. Res. J.*, **57**, 13 (1987); <https://doi.org/10.1177/004051758705700103>.
20. A. Dutta and V.M. Nadkarni, *Text. Res. J.*, **54**, 35 (1984); <https://doi.org/10.1177/004051758405400108>.
21. A.L. Brody, E.P. Strupinsky and L.R. Kline. Active Packaging for Food Applications, CRC press (2001).
22. T.I. Oh, S. Yoon, T.E. Kim, H. Wi, K.J. Kim, E.J. Woo and R.J. Sadleir, *IEEE Trans. Biomed. Circuits Syst.*, **7**, 204 (2013); <https://doi.org/10.1109/TBCAS.2012.2201154>.
23. G.E. Collins and L.J. Buckley, *Synth. Met.*, **78**, 93 (1996); [https://doi.org/10.1016/0379-6779\(96\)80108-1](https://doi.org/10.1016/0379-6779(96)80108-1).
24. R.D. Noble and S. Alexander, Membrane Separations Technology: Principles and Applications, Elsevier, vol. 2 (1995).
25. R. Singh, Hybrid Membrane Systems for Water Purification: Technology, Systems Design and Operations. Elsevier (2006).
26. M.M. Ghobashy and M.R. Khafaga, *J. Supercond. Nov. Magn.*, **30**, 401 (2017); <https://doi.org/10.1007/s10948-016-3718-5>.
27. M.M. Ghobashy, *Ultrason. Sonochem.*, **37**, 529 (2017); <https://doi.org/10.1016/j.ultsonch.2017.02.014>.
28. K. Thamaphat, P. Limsuwan and B. Ngotawornchai, *Kasetsart J. (Nat. Sci.)*, **42**, 357 (2008).
29. R.A.X. Nunes, V.C. Costa, V.M.A. Calado and J.R.T. Branco, *Mater. Res.*, **12**, 121 (2009); <https://doi.org/10.1590/S1516-14392009000200002>.